Metabolic signature of prostate cancer as detected with proton magnetic resonance spectroscopic imaging and 18F-fluorodeoxyglucose-positron emission tomography

Amita Shukla-Dave[1], Cecilia Wassberg[2], Darko Pucar[3], Heiko Schoder[1], Debra Goldman[1], Victor E. Reuter[1], James Eastham[1], Peter T. Scardino[1], Steve M. Larson[1], and Hedvig Hricak[1]

[1]Memorial Sloan-Kettering Cancer Center, New York, New York, United States, [2]Uppsala University Hospital, Uppsala, Uppsala, Sweden, [3]Georgia Health Sciences University, Augusta, GA, United States

Introduction

Although metabolic imaging is frequently performed in patients with cancer, the mechanisms leading to cancer-related genomic and metabolic rearrangements and consequent imaging findings remain poorly understood. Deciphering the links between cancer genomics and metabolism might be essential for improving current imaging modalities and developing new ones in view of the emerging hybrid MRI/PET systems. In prostate cancer (PCa), two key functional imaging modalities, proton magnetic resonance spectroscopic imaging (^{1}H-MRSI) and ^{18}F fluorodeoxyglucose PET (^{18}F-FDG-PET), are based on cancer-induced changes in cellular metabolism[1-4]. ^{1}H-MRSI adds value to anatomic endorectal prostate MRI in the detection, staging of primary tumor, prediction of tumor aggressiveness and recurrent local PCa[5-6]. On the other hand, ^{18}F-FDG-PET is not sensitive for local PCa, and it is most commonly used for the detection of metastatic disease[7]. The purpose of this study was to evaluate citrate metabolism and glucose consumption in prostate cancer using ^{1}H-MRSI and ^{18}F-FDG-PET.

Materials and Methods

This study includes 22 patients [mean age, 59 y; range, 47-70 y; PSA range, 0.11-91.69 ng/mL; biopsy Gleason score range, 6-9] who underwent endorectal MRI/MRSI examinations and ^{18}F-FDG-PET prior to surgery (primary radical or salvage prostatectomy). Whole mount step section pathology was available for all patients. Out of these 22 patients, 11 patients were imaged before treatment while 11 were imaged after external beam radiation therapy (EBRT). The institutional review board approved our retrospective review of MRI/MRSI and ^{18}F-FDG-PETstudies, pathology data (from surgical pathology), and clinical follow-up data and waived the informed consent requirement. Time between MRSI and PET exams was 11±37days (mean±SD). MR data were acquired on a 1.5 Tesla scanner (GE, Milwaukee, WI). The study consisted of MR imaging using a pelvic phased array and expandable endorectal coil followed by standard MRSI protocol with PRESS voxel excitation and water and lipid suppression[8]. The metabolic ratio choline+polyamine+creatine to citrate was calculated for each voxel. All patients underwent combined ^{18}F-FDG PET/computed tomography (CT). Details for these examinations have been described previously[9]. The maximum SUV (SUV_{max}) and the mean SUV (SUV_{mean}) values were recorded for the index tumors. Whole mount step section histopathology was used as the standard of reference. To examine the correlation between the ^{1}H-MRSI data, and ^{18}F-FDG-PET data, Spearman's correlation coefficient (ρ) was used. Only findings with a P value of less than .05 were considered to indicate significance.

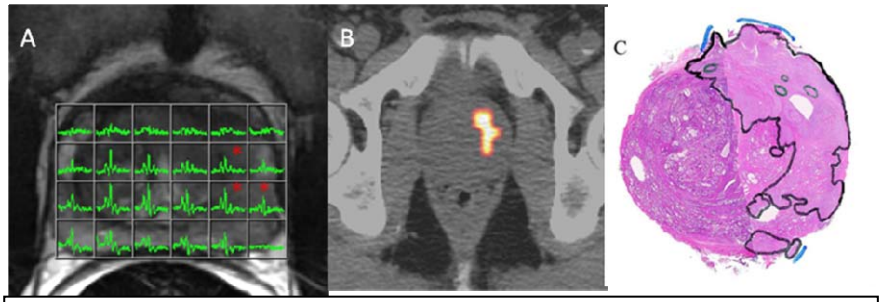

Figure1. Representative 1.5T MRI/MRSI in a 58-year-old patient with PSA 91.69 ng/mL, clinical stage T3 and surgical Gleason score 4+5. A) Axial T2-weighted image and overlaid PRESS box indicating excitation region selected and 3D MRSI demonstrating three suspicious voxels marked with asterisks. B) ^{18}F-FDG-PET/CT fusion image shows a focal uptake in the left prostate. C) Whole-mount step-section histopathology after radical prostatectomy shows a large cancer in the left prostate.

Results

On ^{1}H-MRSI 21 out of the 22 tumors were correctly identified and on ^{18}F-FDG-PET only 3 tumors showed FDG uptake. The 3 tumors positive by ^{18}F-FDG-PET did show changes in citrate as observed by ^{1}H-MRSI. Figure 1 shows ^{1}H-MRSI, ^{18}F-FDG-PET and whole mount step section pathology from a PCa patient in whom the tumor seen at pathology was observed by both imaging modalities. Figure 2 shows ^{1}H-MRSI, ^{18}F-FDG-PET/CT and whole mount step section pathology from a PCa patient in whom the tumor seen at pathology was observed by ^{1}H-MRSI only. The results in the present study suggest that ^{1}H-MRSI changes are seen before the ^{18}F-FDG-PET changes in localized prostate cancer. The total number of suspicious voxels seen by ^{1}H-MRSI ($\rho = 0.549$) and SUV_{max} calculated from ^{18}F-FDG-PET ($\rho=0.756$) for the index lesion significantly correlated with the surgical Gleason score (for both $p<0.01$).

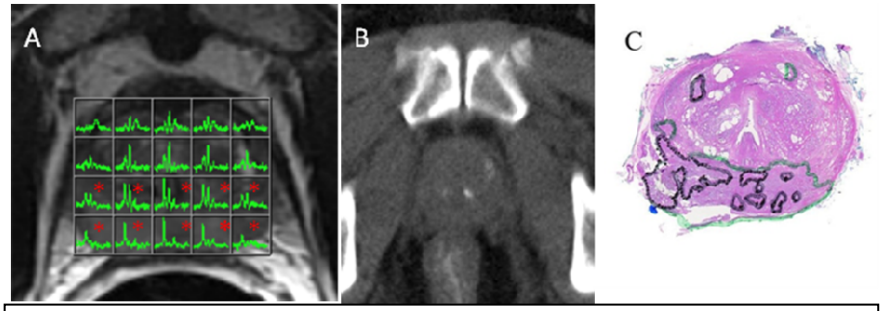

Figure 2. Representative 1.5T MRI/MRSI in a 64-year-old patient with PSA 4.9 ng/mL, clinical stage T3 and surgical Gleason score 4+3. A) Axial T2-weighted image and overlaid PRESS box indicating excitation region selected and 3D MRSI demonstrating ten suspicious voxels marked with asterisks. B) ^{18}F-FDG-PET/CT fusion image shows no focal uptake in the prostate. C) Whole-mount step-section histopathology after radical prostatectomy shows a large cancer extending from medial to right side of the prostate.

Discussion and Conclusion

PCa detection on ^{1}H-MRSI is based on the detection of decreased citrate (a Krebs cycle and fatty acid (FA) synthesis intermediate) and polyamines (amino acid (AA) metabolism intermediates) and elevated choline (a precursor of membrane synthesis)[2,8]. On ^{18}F-FDG-PET, increased glucose uptake by glucose transporters (GLUT) and glucose phosphorylation to glucose-6-phosphate (G6P) by hexokinase (HK) are used for detecting PCa[3,4]. In the present study, since the citrate decrease in PCa as seen by ^{1}H-MRSI was both more frequent and more pronounced than the elevation in ^{18}F-FDG uptake, we suggest that altered citrate metabolism precedes increased glucose consumption in PCa. ^{18}F-FDG-PET is not sensitive for detecting localized primary PCa, and it is most commonly used for the detection and response assessment of metastatic disease[3,4]. Further studies are needed to clearly understand the genomic and metabolic mechanisms leading to changes seen by imaging. This is critical as the basic understanding of these pathways will help us better select the appropriate imaging method or radiotracer for low-risk PCa patients versus those patients that have advanced, metastatic disease.

References [1] Costello LC et al Urology, 1997, 50(1), 3-12. [2] Kurhanwicz J et al, Radiology, 1996, 198 (3), 795-805. [3] Schoder H et al Semin Nucl Med 2004, 34 (4) 274-92. [4] Hoh CK et al J Urol, 1998, 159 (2), 347-56. [5] Sciarra A et al Eur Urol 2011, 59 (6), 962-77. [6] Mazaheri Y et al J Magn Reson Imaging 2011, 33(2), 258-74. [7] Schoder H et al Clin Cancer Res 2005, 11 (13), 1387-98. [8] Shukla-Dave A et al Radiology, 2007, 245 (2) 499-506. [9] Meirelles GS et al Clin Cancer Res 2010, 16 (24), 6093-9.